

# Experimental method of optical coherence characterization in phase-space measurement

Jie-En Li\*, Jhih-Syuan Fu, Ming-Shu Hsiao, and Chung-Hao Tien

Dept. of Photonics, National Chiao Tung University, 1001 University Road, Hsinchu, Taiwan 300, ROC

## ABSTRACT

A novel approach of phase-space measurement made its debut with the experimental result. We first designed an experiment based on the Young's interferometer to characterization the optical coherence property of light source. A well-known algorithm called Hough transformation was applied to deal with the misalignment of micro-lens array by post-processing. The phase-space image of plane wave was then reconstructed from the realigned raw image. Finally, the properties of this system were discussed.

**Keywords:** Phase-space optics, Coherence, Statistical optics, Micro-lens array.

## 1. INTRODUCTION

A novel approach of phase-space measurement which is able to record the position and angular spectrum of optical field at once makes its debut with the experimental result. By applying the statistical nature of light, the mutual intensity function provide a huge amount of information of partially coherent field [1-2]. The mutual intensity function can be measured by the Young's interferometry, which allows us to obtain the degree of coherence from the fringe visibility [3]. Nevertheless, the process of pixel-by-pixel scanning costs a lot of time and the performance suffers greatly from the mechanical calibration. Another approach is phase-space tomography, which allows us to accelerate the measurement by scanning along the optical axis instead of under appropriate boundary conditions [4-5]. However, it usually takes lots of computational work so that it is necessary to find another way.

In order to overcome these issues and measure the information of partially coherent field in simple and efficient way, a brand new method of phase-space measurement is proposed by L. Tian *et al* recently [6]. By placing the imaging sensor at the back focal plane of the micro-lens array, we are able to record the angular spectrum of each localized space as shown in the Fig. 1.

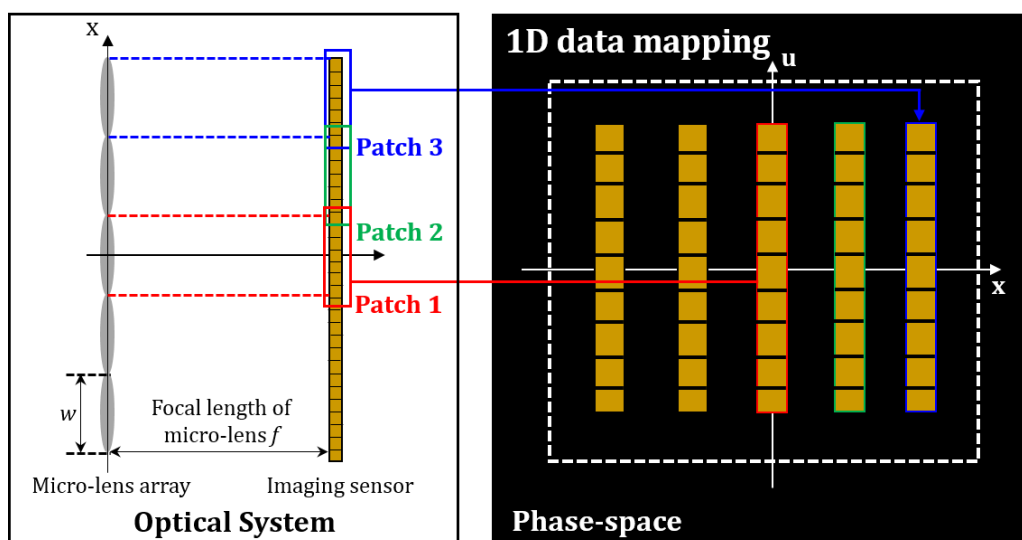


Figure 1. Illustration of one dimensional data mapping. The imaging sensor is placed at the back focal plane of the micro-lens array. The diameter and focal length of each micro-lens are  $w$  and  $f$ .

\*jaen88617.eo01g@nctu.edu.tw; phone 886-3-5712121-59209; fax 886-3-5735601

Optical Systems Design 2015: Computational Optics, edited by Daniel G. Smith, Frank Wyrowski, Andreas Erdmann, Proc. of SPIE Vol. 9630, 96300D · © 2015 SPIE  
CCC code: 0277-786X/15/\$18 · doi: 10.1117/12.2190413

However, the size of each patch which contains the information of angular spectrum is related to the specification of micro-lens, the diameter  $w$  and focal length  $f$ . According to their discussion, the cross-talk of each patch can be mainly divided into two part. The 0<sup>th</sup>-order cross-talk is induced by the incoherent properties of light. The other one is influenced by the coherent phenomena of light called high-order cross-talk. They also provide an optimal region for designers as a guideline in their work, as shown in the Eq. 1.

$$0.02w < \sigma_c < 0.4w. \tag{1}$$

The parameter  $\sigma_c$  is a coherent quantity of Gaussian Schell model beam [Eq. 15, Ref. 6]. This result allows us to determine the specification of micro-lens with minimum cross-talk. Unfortunately, previous work only stays in simulating stage and there is no further experimental result about this phase-space measurement system.

Therefore, in this work, we want to realize their proposal of phase-space measurement. At the beginning stage, we first construct an optical system which is based on the Young’s double-slits interferometer to characterize the spatially coherent property of light source. Unlike another work, a positive lens is placed among the conventional interferometer to manipulate the imaging size of coherent area [7]. As we shifting the positive lens along the optical axis, different magnification of coherent area pass through the relaying lens. The interferograms is captured by the imaging sensor and the degree of coherence is determined by the fringe visibility as usual. By applying the algorithm of regression, we can find the spatially coherent property  $\sigma_c$  of our system. The optimal region of the diameter of micro-lens in our phase-space measurement system is around 8.27  $\mu\text{m}$  to 165.25  $\mu\text{m}$ . The preliminary result of phase-space image will be given in the following section.

## 2. METHODOLOGY

The experimental setup of optical coherence characterization is shown in the Fig. 2. Assuming the original light source is ergodic and stationary at least in the wide-sense. Since the central wavelength of this source is 635 nm and the spectral bandwidth is less than 10 nm, we can treat it as a quasi-monochromatic light. A pinhole with 25 $\mu\text{m}$  diameter combining with a collimated lens can be regarded as our secondary light source, whose optical coherent property is the target we are going to deal with.

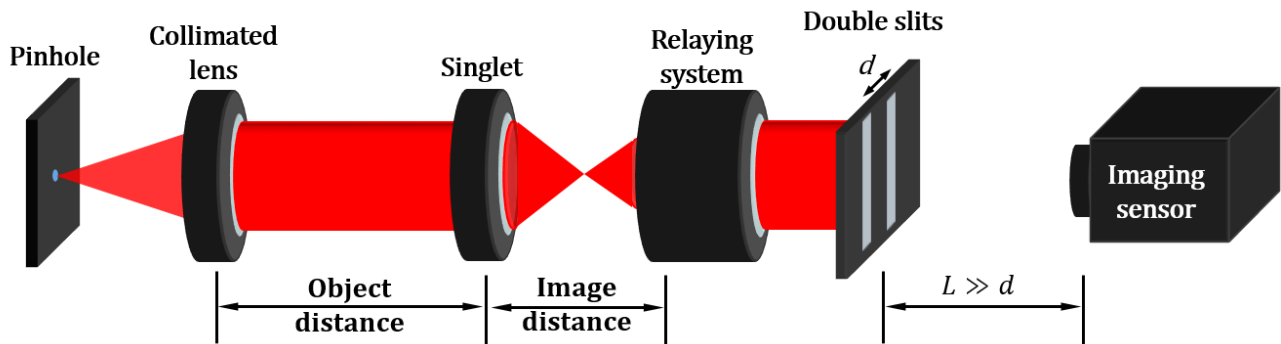


Figure 2. Experimental setup of optical coherence characterization. The singlet among the interferometer controls the image of the coherent area.

Suppose the optical coherent property consists with the Gaussian Schell model as below.

$$\gamma(d) = \exp \left[ - \left( \frac{d}{\sigma_c} \right)^2 \right]. \tag{2}$$

The remaining problem becomes measuring the degree of coherence under different slits distance  $d$  and finding the parameter  $\sigma_c$ . However, we can only acquire a fixed portion of  $\gamma(d)$  in the original Young’s interferometer when the distance  $d$  of double slits is fixed. And this constraint make the works of regression, which we used to tackle the problem of finding  $\sigma_c$ , awkward because this problem has infinite number of solutions. In order to overcome this issue, we add a singlet among the conventional setup. The role of this singlet in this experiment is an imaging system, which provides an image with additional magnification depending on situation. According to the lens-maker’s formula, the magnification of image is defined by the ratio of image distance to object distance, as shown in Eq. 3.

$$M = \frac{\text{Image distance}}{\text{Object distance}}. \quad (3)$$

By tuning the magnification of this system, we can control the spot size of incident wave at the entrance pupil of relaying system. Hence, Eq. 2 can be rewritten as a function of dimensionless quantity  $c$ , which represents the ratio of the slits' distance  $d$  to spot size.

$$\gamma^* \left( c = \frac{\text{distance of double slits}}{\text{spot size at entrance pupil}} \right) = \exp \left[ - \left( \frac{c \cdot D}{\sigma_c} \right)^2 \right]. \quad (4)$$

The parameter  $D$  is the spot size of object field and  $\gamma^*$  is the degree of coherence by the measurement. As a consequence, our target of curve fitting becomes a function of  $c$ , which implies the optical coherent property inside that spot. In other words, the target function we have to tackle can reveal how much the degree of coherence the wave is at different position within the spot. For example, a complete coherent spot means the measured degree of coherence equals to 1 when  $c$  is larger than 1. On the contrary, a partial or incoherent spot can be called if  $\gamma^*(c < 0) = 1$ , depending on the situation.

Above experiment allows us to determine  $\sigma_c$  of the secondary source we are going to use in the following phase-space measurement. Once we obtained the coherent property of source, we can start to measure the phase-space with minimum expected noise. The experimental setup of phase-space measurement system is shown as below.

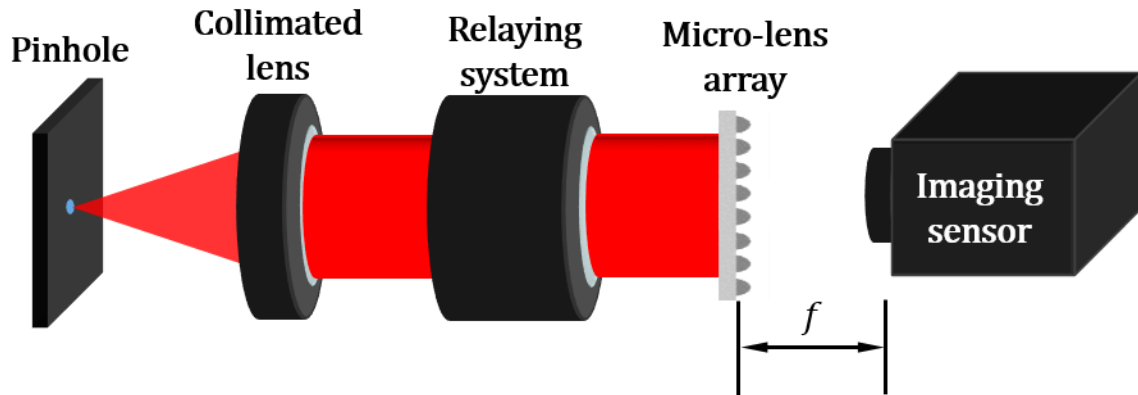


Figure 3. Experimental setup of phase-space measurement. A micro-lens array is added in front of the imaging sensor. In order to acquire the localized angular spectrum of each micro-lens, the imaging sensor has to place at the back focal plane of the micro-lens array.

As we mentioned before, the first two component on the left-hand side produce a collimated light source with less spatial noise. This collimated field then passes through the relaying system and illuminates onto the micro-lens array. Because the information of phase-space is in the joint space/spatial-frequency domain. The imaging sensor has to place at the back focal plane of the micro-lens array. Each micro-lens locally transforms the field in space domain into spatial-frequency domain. The result angular spectrums of every micro-lenses are recorded by the imaging sensor.

We have shown the schematic diagram of 1D data mapping. Nevertheless, most of optical waves we have to deal with in real world are two dimensional field. This fact causes a four dimensional information in the joint space/spatial-frequency domain. The variables in the four dimensional space are listed in the Table 1.

Table 1. List of variables in the joint space/spatial-frequency domain.

Variables	Description
$(x, y)$	Spatial coordinates
$(u, v)$	Spatial frequency coordinates

The entire four dimensional information is now recorded in a two dimensional image. The next issue becomes to decode this image and reconstructs the phase-space. Before we present the result of reconstructed phase-space image. There has another sub-issue that is worth our while to introduce as shown in the following figure.

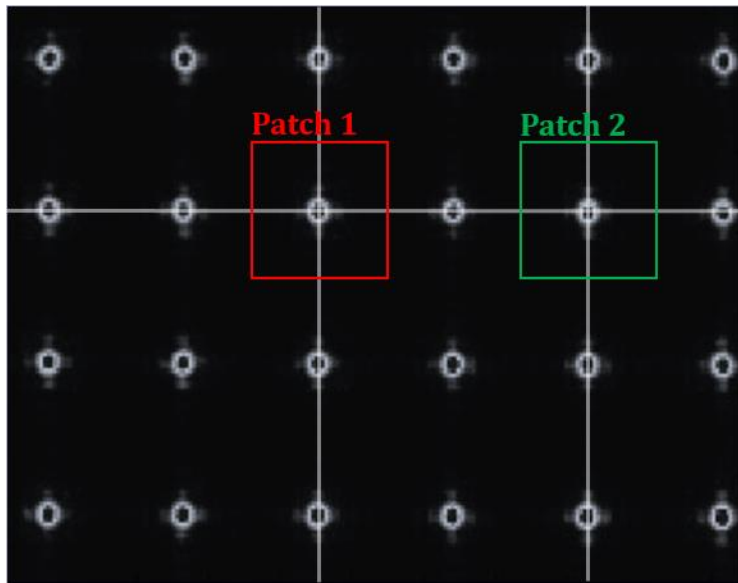


Figure 4. Alignment issue in the phase-space image. Two patches of angular spectrum are marked by the red and green frame. The centers of these two patches seem to have a slight shift compared to the grid lines (gray lines).

Figure 4 shows the phase-space image captured by our system. Two patches of angular spectrum formed by the micro-lens are marked by the red and green frame. The centers of these two patches seem to have a slight shift compared to the grid lines. This issue is induced by the misalignment of micro-lens array along the  $\varphi$ -axis on the transverse plane. As a consequence, it causes the grid lines rotate around the optical axis slightly. Typically, the rotation angle of this issue is usually in several milli-radian. However, this several milli-radian will severely affect the reconstruction process.

In order to solve this issue, we apply the well-known Hough transformation to detect the rotation angle of grid lines [8-9]. The objective of this issue is pursuing the most suitable curve for connecting every centers of the patches. Fortunately, the micro-lens array we used is rectangular packed. Therefore, the target becomes a straight line with unknown slope and distance as below.

$$x_0 \cos \theta + y_0 \sin \theta = r. \tag{5}$$

The variable  $r$  is the distance from the origin to the closest point on the line that is defined by Eq. 5.  $\theta$  is the angle between the  $x$ -axis and the normal vector of the line. By compiling the statistics  $(r, \theta)$  of every centers, we can obtain the most possible solution sets  $(r_h, \theta_h)$  and  $(r_v, \theta_v)$ , which represent the horizontal grids and vertical grids, respectively. The results of Hough transformation will be given on the following conference. The reconstruction result of phase-space image will be shown in the next section.

### 3. RESULTS AND DISCUSSIONS

Previous section describes all the preparations and techniques to get a phase-space image with a snapshot. After the optical coherence characterization of the light source, we choose a micro-lens array with 146  $\mu\text{m}$  lens diameter and 150  $\mu\text{m}$  lenslet pitch. The two dimensional image is then digitally realigned by Hough transformation. By applying the two dimensional data mapping, which is based on the concept of one dimensional data mapping. The reconstruction result of a plane wave image in phase-space is shown in the Fig. 5. Because of the down-sampling effect of the micro-lens array, the resolution of this image is only  $54 \times 20$ , 54 pixels in spatial coordinate and 20 pixels in spatial frequency coordinate. Each pixels represents 150  $\mu\text{m}$  in horizontal domain and  $2.43 \text{ mm}^{-1}$  in vertical domain. The

result in phase-space shows the intensity profile of the incident wave in spatial domain is uniform and the divergent angle is approximately  $6.16 \times 10^{-3}$  rad, which has a good agreement with the characteristic of plane wave.

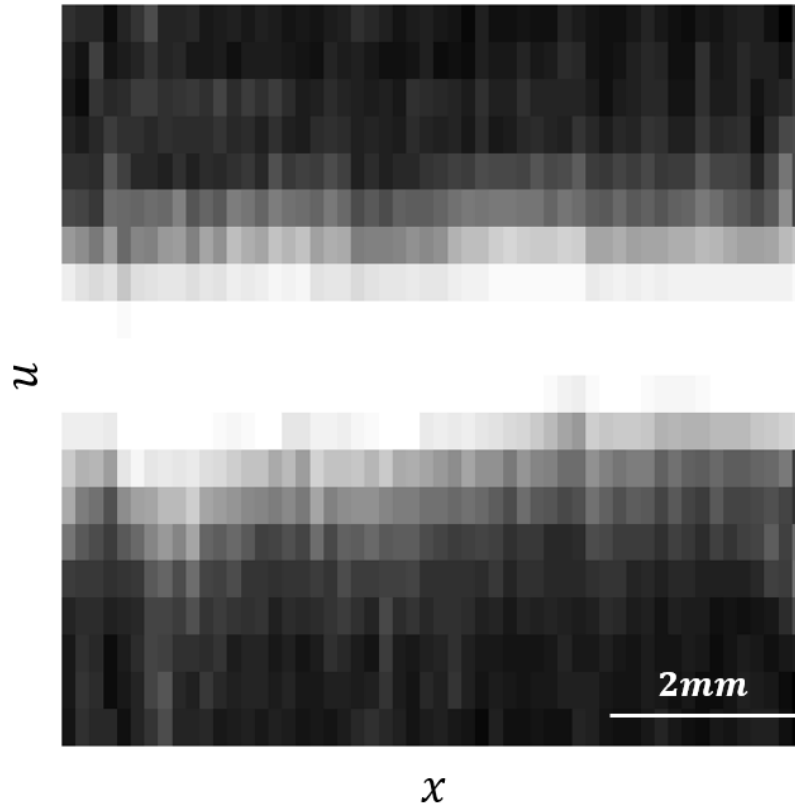


Figure 5. Reconstruction result of  $x-u$  image in phase-space. The incident wave is a plane wave with 635 nm central wavelength.

However, there are two defects in this system. Since we store four dimensional information in only two dimensional space, the first one becomes the down-sampling issues in spatial domain due to the intrinsic limitation of micro-lens. This issue might be solvable by applying the technique of super-resolution algorithm under proper circumstances which will not cost too much time. The second one is about the frequency response of this system. The maximum frequency we can acquire in this system is related to the numerical aperture of the micro-lens and the sampling frequency of the imaging sensor. For example, the numerical aperture of micro-lens we used in this experiment is about 0.02, which leads to a constraint on the cutoff frequency. According to the diffraction-limit, the cutoff frequency of this system is  $31.50 \text{ mm}^{-1}$ . That means we cannot capture a phase-space image whose spatial frequency is beyond the cutoff frequency, such as a lens.

#### 4. CONCLUSIONS

In this work, we first consult the idea of measuring the phase-space image by placing a micro-lens array in front of the imaging sensor proposed by L. Tian *et al.* Then we construct the first experiment based on the Young's interferometer to characterize the optical coherent property of the light source. In order to realign the raw image of the second experiment, we use the Hough transformation to determine the grid lines. The phase-space image of a plane wave was then reconstructed according to the realigned raw image. Finally, we discuss the two major limitations of this system. Although the issue of limited cutoff frequency seems to have no solution today, it doesn't mean there will never have an answer in the future.

#### 5. ACKNOWLEDGEMENT

The financial support from the Ministry of Science and Technology, Taiwan under contract NSC 102-2221-E-009-115-MY3 is acknowledged.

## REFERENCES

- [1] Goodman, J. W., [Statistical Optics], John Wiley & Sons, New York (1985).
- [2] Wolf, E., [Introduction to the Theory of Coherence and Polarization of Light], Cambridge University Press, New York (2007).
- [3] Thompson, B. J. and Wolf, E., "Two-beam interference with partially coherent light," *J. Opt. Soc. Am.* 47(10), 895-897 (1957).
- [4] Raymer, M. G., Beck, M. and McAlister, D., "Complex wave-field reconstruction using phase-space tomography," *Phys. Rev. Lett.* 72(8), 1137-1140 (1994).
- [5] Tian, L., Lee, J., Oh, S. B. and Barbastathis, G., "Experimental compressive phase space tomography," *Opt. Express* 20(8), 8296-8308 (2012).
- [6] Tian, L., Zhang, Z. and Barbastathis, G., "Wigner function measurement using a lenslet array," *Opt. Express* 21(9), 10511-10525 (2013).
- [7] Divitt, S., Lapin, Z. J. and Novotny, L., "Measuring coherence functions using non-parallel double slits," *Opt. Express* 22(7), 8277-8290 (2014).
- [8] Hough, P. V. C., [Methods and means for recognizing complex patterns], U.S. Patent 3.069.654, 1962.
- [9] Duda, R. O. and Hart, P. E., "Use of the Hough transformation to detect lines and curves in pictures," *Commun. ACM*, 15(1), 11-15 (1972).